Thermophysical Model to Numerically Determine the Diffusivity of Highly Excited Nuclear Matter with an Instantaneous, Internal Pulse Method†

Harald Reiss*,‡ and Oleg Yu. Troitsky§

Department of Physics, University of Wuerzburg, Am Hubland, D-97074 Wuerzburg, Germany, and Department of Applied Computer Science, Seversk State Technology Academy, 65 Kommunisticheskiy Avenue, Seversk, Tomsk Region 636036, Russia

We have studied thermalization of binding energy released as an instantaneous, internal heat pulse in a sphere. This resembles transient heat transfer in laser flash experiments, where thermal diffusivity is determined from temperature evolution measured on front or rear surfaces of thin films. Here, instead, we are interested in the long term behavior of sample temperature when it approaches thermal equilibrium. The method is applied to a nucleus. Therefore, not only energy source, time scale, and sample geometry but also materials, properties, and boundary conditions in the present article are completely different from conventional matter and standard laser flash methods. However, the principle by which determination of diffusivity is made is conserved. Diffusivity, κ, of the nucleus is estimated from kinetic gas theory to be $\kappa/[10^{-8}\ m^2 \cdot s^{-1}] = 9.35 \pm 2.97$. Second, numerical simulation yields the time, t_E, needed for thermalization after the disturbance. From comparison of t_E with lifetime resulting from the uncertainty principle, the diffusivity can be extracted. Both results for κ agree within 10 %, but κ depends on energy level density (or excitation energy), a dependence that is not reported in previous literature. Thermalization in nuclear matter is confirmed to proceed by diffusion. The new internal source method could be transformed to experiments on a laboratory scale.

1. Introduction

Laser flash experiments apply transient conduction heat transfer as a tool to extract thermal properties of thin film materials. An instantaneous heat source is generated by absorption of a laser pulse on a flat, heat-conducting, nontransparent sample. The diameter of the heat source should be large compared with the sample thickness to establish approximately 1D heat flow. Thermal diffusivity of the sample is determined from temperature evolution with time measured on its front or rear surfaces; data are taken shortly after the end of, or even during, the radiation heat pulse.

Laser flash belongs to a series of unsteady-state measurement methods that can be grouped according to the nature of the specific disturbance into pulse, periodic heat flow, and monotonic heating regime methods. The most recently developed of these, the pulse method, has gained much popularity among thermophysicists in the last four decades because of the ease with which initial and boundary conditions of the mathematical heat conduction model can be reproduced in a physical experiment, the simple shape of the specimen, and the wide range of materials, diffusivities, and temperatures to which the method is applicable. The very short bursts of radiant energy traditionally are emitted from a laser or from a xenon flash lamp.

As a transient energy source, single particles or pulsed beam of particles (electrons or ions) can be used as well. In the present article, the method is generalized to another type of energy source, that is, localized release of binding energy, which extremely short duration of the pulse, in comparison to traditional methods.

Whereas in standard laser flash experiments, focus is on transient aspects of the diffusion process, in the present article, we are interested in the long-term behavior of sample temperature, and diffusivity will be extracted using a numerical model from the time needed to obtain thermal equilibrium within a sphere.

Thermalization means a process to distribute energy to all constituents of a solid, liquid, or gaseous system; this means that the constituents of the system finally arrive at a Maxwellian velocity distribution. Consider a gas enclosed in a spherical, gas-tight container. Let a heat pulse be released at arbitrary positions in its interior. Furthermore, assume that the internal pressure is high enough that the mean free path between collisions of gas molecules is small in comparison with the diameter of the spherical volume. The gas molecules will then quickly distribute their excess energy by particle/particle collision, which means that there is a diffusionlike, stepwise process to distribute this energy to all constituents. To find a mathematical solution to the spherical conduction problem, one would naturally consult Carslaw and Jaeger,[1] chapter X, for an instantaneous point source or for instantaneous surface sources of finite dimensions in infinitely extended or semi-infinite, or chapter XIV, for finite regions. However, as will be shown later, we need a solution for an instantaneous volume source positioned at arbitrary locations in a heat-conducting region of finite dimensions. Therefore, numerical solutions have to be investigated. One may argue that determination of the time needed to reach equilibrium in finite volumes and, accordingly, the extracted diffusivity would strongly depend on dimensions of source and sphere, but we will select an exotic sample where this is not the case.

* Corresponding author. Address: P.O. Box 25 13 37, D-69080 Heidelberg. E-mail: harald.reiss@physik.uni-wuerzburg.de. Fax: +49 6221 80 44 32.
† Part of the "William A. Wakeham Festschrift".
‡ University of Wuerzburg.
§ Seversk State Technology Academy.

10.1021/je9000334 CCC: $40.75
Published on Web 04/29/2009

Heat transfer in spheres is rarely studied, such as heating of chemical fluids in spherical containers or heat losses from large, spherical, thermally insulated cryogenic storage units. Symmetry relations are usually exploited to simplify the description of temperature excursion within a sphere. Only a few applications require rigorous treatment of heat transfer in spherical coordinates, such as evaporation of water droplets on a hot surface (the Leidenfrost state) or radiation losses from hot air balloons to the atmosphere (both examples do not exhibit rigorous spherical symmetry).

It is hardly possible to find an appropriate spherical system that on the one hand shall allow rigorous treatment of thermalization solely by conduction after release of a heat pulse and on the other hand represent a meaningful technical application or an illustrative theoretical example that improves understanding of heat transfer or helps to establish a new experimental method. The system, unlike a gas at constant pressure or a liquid volume of constant spherical geometry should not need a vacuum-tight container or other boundaries to "freeze" its spherical shape. A mercury-in-glass thermometer with a spherical bulb, as suggested in ref 1, p 235, initially at temperature $T = 0$, that is, plunged at time $t = 0$ in a medium at $T > 0$, would not be a good example because it neither approaches an arbitrarily located, single, pointlike heat source nor can thermal expansion of the mercury be neglected. Superinsulated, spherical cryogenic containers are hollow spheres with a stored liquid that would not distribute heat just by conduction; instead, there is also free convection, and cryogenic storage units usually are not exposed to irregular working conditions such as an instantaneous heat source on its surface.

But there are perhaps other more exotic candidates that could be investigated with methods analogous to standard laser flash? A possible example is the Earth, or a stellar atmosphere, that is hit by an incident celestial body. However, both spheres continuously suffer radiation losses to space that have to be compensated by internal energy sources (decay of unstable nuclei in the Earth, fusion of light elements in a stellar atmosphere). But traditional laser flash methods are not applied to samples with internal generation of heat. Therefore, also, these two exotic candidates are ruled out.

We finally selected the nucleus: This system is spherical by virtue of its strong, attractive nuclear potential; the special case of deformations from spherical symmetry occurring under rotation or vibrations will not be considered. A nucleus in some aspects behaves like an ideal gas, as will be discussed later. A compound nucleus, one of the most interesting many-particle systems that can be formed in energy-releasing target/projectile collisions, reaches thermal equilibrium without any interaction with its surroundings, with incident kinetic and release of binding energy at any location in its volume or on its periphery. (Precompound emissions, too, are not considered in this contribution.) The reader, firm in laser flash methods but perhaps not familiar with nuclear physics, will agree in the following that a compound nucleus is an ideal system for investigating thermalization by a thermophysical model by analogy to laser flash methods.

Once it is shown in the next sections that an internal energy source such as release of binding energy instead of absorption of radiation or particle energy from external sources can be successfully applied to a sample (here the nucleus), the question is whether this result has some significance to experimental application also on a laboratory scale. Yes, a chemical reaction or radioactive decay of an appropriate nucleus with a lifetime not too short, both introduced as "tracers" at appropriate positions, would be tempting examples. However, an experimental check of the method on a laboratory scale has to be shifted to a later date.

Accordingly, in this article, transient energy source, sample geometry, and time scale as well as materials properties and boundary conditions are completely different from usual laser flash experiments and conventional matter. However, the basic principle for determination of diffusivity by standard laser flash methods is also conserved in the present case: We have (a) a heat conducting sample (here the nucleus), (b) a heat pulse as a probe (here binding energy suddenly released at a specific location), and (c) a detector that measures temperature evolution with time. (In the present case, it is the numerical simulation that yields the time needed by the nucleus to reach thermal equilibrium.)

Although this coincidence seems to be encouraging, we will in the first steps more tentatively apply transient heat conduction to nuclear matter to determine its diffusivity. It is not at all clear that thermalization of energy in such an exotic case proceeds by the same rules as that in classical condensed matter. There, energy is distributed by solid particle/particle collisions or radiative transfer; here the mechanism of nucleon/nucleon interactions in a nuclear volume (collisions, in a classical sense?) has to be thoroughly discussed. Strictly speaking, the method for determining diffusivity of nuclear matter, as described in the following, is not limited to thermalization in compound nuclei. A description of a collision process, with a projectile impinging at high beam energies on a target nucleus and modeling dynamic processes and competing reactions (direct reactions, precompound emissions) involved until equilibrium (if possible) is obtained would be an alternative, but a very complicated one in comparison with a comparatively simple event such as release of binding energy. In other words, the compound nucleus here serves as an illustrative vehicle for handling physics (mostly energy balances) as simply as possible.

However, in any system, distribution of energy needs a transport mechanism. If energy transfer in nuclear matter would be realized like that in its classical condensed counterparts (collisions, usually with a mean free path that is small in relation to volume dimensions), then it would resemble classical conduction without radiative contributions. At least the last condition seems to be fulfilled: In a nucleus, single nucleons do not exchange radiation, neither with other constituents of the same nucleus nor with its surroundings, because protons and bound neutrons are stable particles. Whereas γ emission, too, de-excites a nucleus, it is not clear that it would initiate a diffusion process originating from a localized, transient energy source. Yet the question of whether a diffusion model is applicable to nucleon/nucleon interactions to distribute energy is provisionally left open until the discussion in Section 4.

Following the scheme a−c, the next question is, "What is the nature of a transient energy source that could be thermalized in a compound nucleus?"

2. Compound Nucleus Reaction Model

2.1. Nuclear Reaction Channels. We will first describe some basic aspects of a compound nuclear reaction. Assume that a projectile particle, A, composed of single nucleons (neutrons and protons) hits a target nucleus, B, at an incident kinetic (center of mass) energy high enough to overcome Coulomb repulsion between A and B. Besides competitive reaction mechanisms, the nuclei A and B can merge to an intermediate system ($A + B$), the compound nucleus (CN). Assuming that a nucleus consists of nucleons as if they were solid particles is

somewhat naïve. It is more realistic to assume that the constituents of the nucleus are quasi-particles. Their properties are similar to those of nucleons if they reside near the Fermi level of the whole system. The difference between Fermi energy and the depth of the nuclear potential is comparatively small, which means nuclei are weakly bound systems.

As a simple example, assume that a target nucleus, ^{10}B, is hit by a projectile, ^{4}He (an α particle consisting or two protons and neutrons; the upper indices indicate the total number of single nucleons forming the nuclei). Complete fusion of target (boron) and projectile (α particle) results in the formation of an intermediate, that is, a compound nucleus composed of, in total, $A = 14$ nucleons, ^{14}N, by conservation of mass and electrical charge. After its formation in the entrance "channel" $A + B$, the compound nucleus approaches thermal equilibrium before it decays into different decay channels, $C + D$. It "evaporates" different kinds of particles, C, such as neutrons (n) or protons (p). Evaporation of n or p relieves the residual nucleus, D, here ^{13}N or ^{13}C, respectively, in its ground or excited energy states. Details will be discussed below; we will later also focus on compound nuclei composed of a much larger number of nucleons to apply statistical mechanics safely. (Under this condition, deuterons or heavier particles could also be released.)

Thermalization in a CN, following its formation, is completed after about 10^{-16} s; after this period, the CN decays. (We will later discuss where this time comes from.) The period 10^{-16} s is very long in comparison with time scales of other nuclear reactions (about 10^{-22} s for an incident particle to fly across the volume of a nucleus or for "direct" particle transfer reactions such as strip or pickup). Bohr accordingly said that the compound nucleus, after having obtained thermal equilibrium, "forgets" how it was produced. This means that once the compound nucleus is formed and thermalization is completed we no longer can identify initial projectile, A, or target nucleus, B, and the individual particles of which both projectile and target nucleus were composed from properties of the compound nucleus or from any of its decay products, $C + D$. Thermalization also means increase in entropy of the compound to a relative maximum and corresponding loss of information about previous states and history of formation. There are similar cases where after thermalization of any form of energy, including radiation, the final system does not allow identification of initial states. In nontransparent media, for example, radiative transfer can be described as a conduction process; also, here entropy production is maximum,[2] and we cannot identify from scattered or remitted radiation whether the source was diffuse or directional. Entropy production during the formation of a CN thus has some relatives in other fields. This means that the CN, ^{14}N in the present example, could also be formed in reactions such as $^{12}C + d$ (a deuteron, d, consists of 1 n and 1 p). It even implies that entrance and decay channels can be interchanged and the kinetic energy in the corresponding entrance channels can be properly adjusted to yield the same compound nucleus in the same states of energy with different yield rates, however. Accordingly, the CN could also be excited in reactions such as $^{13}N + n$ or $^{13}C + p$ (just the reverse of the original decay channels in the present example).

2.2. Energy Balance of Compound Nuclear Reactions. Qualitatively, the energy balance of compound nucleus formation and its decay can be described with a liquid drop model in that "droplets", A and B, of the entrance channel collide and fuse and thus supply energy to the intermediate "droplet" CN, which, accordingly, is heated to a high temperature. The compound nucleus during formation accordingly can be assigned

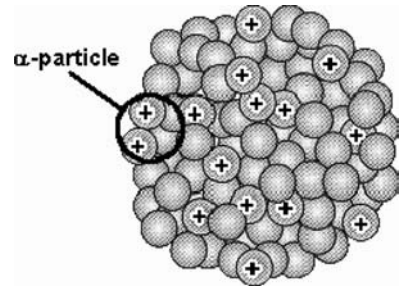

Figure 1. Schematic description of a nucleus. Neutrons (zero total electrical charge), protons (with + inside), and the formation of an α particle (two neutrons, two protons) at the periphery are shown. The Figure has been taken from ref 4 but is slightly modified. Reprinted with kind permission of Springer Science + Business Media.

a defined excitation energy, E^*, which in the reaction $A + B \rightarrow CN^*$ is supplied by the kinetic energy (E_{cm}) in the center of mass (cm) system "projectile plus target" and from release of binding energies, E_B, in the entrance channel, A and B.

The corresponding energy balance is given by

$$E^*_{CN} = E_{cm} + Q \tag{1}$$

where Q is the "Q value", that is, the sum of binding energies of the nuclei concerned in the entrance channel. Examples will be given later.

Variation of E_{cm}, assuming the same projectile and target nuclei in the entrance channel (i.e., keeping the E_B of this channel constant), accordingly produces excitation energies at different height, E_{CN}^*. If E_{cm} and E_B are given, then the CN has a defined E_{CN}^*. A "spectrum" of excitation energies of the CN thus can be fabricated if E_{cm} is slowly increased by measuring "excitation functions", but individual measurements always produce only a single E_{CN}^*.

Conversely, decay of the droplet CN* by evaporation of single nucleon or heavier droplets, $CN^* \rightarrow C + D$ serves for cooling of the CN because the decay products carry away some kinetic energy in the center of mass system of the exit channel, C and D.

Excitations of a liquid drop are usually explained by vibrational states of energy, but Tomonaga[3] already pointed out that the viscosity of nuclear matter is so high that any vibrations of a corresponding liquid drop would aperiodically be damped, which means that stationary excited states of neither a conventional liquid drop nor a nucleus can be interpreted as vibrations of single constituents. But averages, taken over partial or total number of constituents and vibrational states, allow estimates of level density and, as we will see later, specific heat of nuclear matter.

Decay products may be emitted from the CN if they statistically gain enough energy to penetrate (tunnel) the potential barrier of the CN that keeps all nucleons together. Because it is a statistical process, decay of the CN* favors emission of nucleons or heavier particles at the smallest possible energy. If the decay products are charged, then this energy is given by the Coulomb barrier of the CN*, the threshold against emission.

Because the CN, before its decay, is considered to be a gaslike system of individual particles (nucleons, i.e., neutrons or protons), particles heavier than single nucleons first have to be formed in the CN before they can be emitted. (Justification of considering a nucleonic "gas" will be discussed in the following sections.) Such particles, for example, α particles, may be formed anywhere in the CN, either near the surface (as schematically indicated in Figure 1, from ref 4, p 113) or deep

in its interior. Particle formation in the CN also obeys statistical rules. For example, the probability of the formation of an α particle with energy E_α is in proportion to the inverse number of possibilities of distributing the residual energy $E^* - E_\alpha$ to the remaining A-4 nucleons, the residual nucleus, *D*. The A-4 nucleons accordingly will occupy a very large number of different energetic states. The number of levels is thus representative of the number of states to which $E^* - E_\alpha$ can be distributed. The higher E^*, the more competing modes of deexcitation become available for this level.

When a particle that is heavier than a single nucleon is formed in the CN, binding energy, E_B, is released as an energy pulse, which will be delivered to the CN before the particle is evaporated. In the case of the α particle, E_B is comparatively large (28.29 MeV; 1 eV = $(1.602 \cdot 10^{-19})$ J).

It is the binding energy, E_B, that in the following will constitute the instantaneous energy source needed to determine the diffusivity of the CN from simulation of its temperature excursion with time. Because the α particle occupies a small but finite volume, a numerical method for analyzing thermalization requires modeling not of a surface but of a volume source located at any position inside the compound nucleus.

Like other many-particle systems, an excited nucleus can be assigned a temperature by application of statistical mechanics. How can we specify "nuclear temperature"?

2.3. Nuclear Temperature. Consider again the sample CN reaction of Section 2.1 where ^{14}N was formed as the CN in the reaction of ^{10}B (target) with an α particle (projectile). Let E_{CN}^* and E_D^* indicate the excitation energy of the compound nucleus and the excited energy levels of residual nucleus, *D*, respectively. To "populate" the levels E_D^*, including their ground state (the lowest excitation energy, $E_D^* = 0$), the E_{CN}^* must be large enough to satisfy the corresponding energy balances of the exit channel. Compare Figure 2a (from ref 5, p 58): The ground state of the residual nucleus, ^{13}C, is populated by the emission of a proton from ^{14}N. Any state of ^{13}C can be populated only from energy levels of the ^{14}N located at least at the same height in this diagram. (For simplicity, vertical positions of the ground states of the two residual nuclei displayed in Figure 2a, on the energy scale, have been adjusted relative to the ground state of the ^{14}N.) Population of the ground state of ^{13}C means that the emitted proton would be given the maximum kinetic (center of mass) energy available, whereas excited states of ^{13}C would consume some of the energy from the entrance channel, and the corresponding kinetic energies of the protons would, accordingly, be reduced.

It is thus clear from Figure 2a that "discrete" energy levels such as the ground state ($E^* = 0$) and the states at $E^* = (2.31$ and 3.95) MeV excitation energy of the CN cannot decay by emission of p or n to any of the levels of the residual nuclei ^{13}C and ^{14}N simply for energetic reasons; these "bound" states decay only by emission of γ quanta or by internal conversion as a competing process. There are other "selection rules" that also correspond to conservation of angular momentum and parity that can be neglected in the present (energy-related) discussion. Location on the energy scale of bound states above the ground state of a nucleus are usually described by the nuclear "shell model". (See standard volumes on nuclear physics such as refs 4, 5, 6, 7, and 8.)

With increasing excitation energy, however, the number of levels E_{CN}^* increases so that at excitation energies that exceed dissociation energy, a variety of levels E_{CN}^* by decay can populate energy levels in the residual nuclei; these are called "virtual" levels. For example, the virtual level at $E_{CN}^* = 13.71$ MeV can decay to the $E_D^* = 2.365$ MeV and the ground state of ^{13}N, but decay to the level at 3.51 MeV of ^{13}N* is forbidden by conservation of energy. Discrete states are no longer observed in the excitation function at these high E_{CN}^*, instead a continuum of excitation energies, with a density $\rho(E_{CN}^*)$, is created.

A density function, $\rho(E^*)$, describes the distribution of excited energy levels the better the higher the excitation energy and the larger the number of nucleons, *A*. A description of the few bound states of ^{14}N in Figure 2a by a level density formula would make no sense. For this reason, we will in the following consider nuclei with $A = 100$. For example, if $Z = 44$, it is a Ruthenium nucleus. Such a "statistical model" is generally considered to be a valid concept for nucleon number $A > 30$.

The level density at high excitation energies can be calculated using expressions given in a standard textbook on nuclear physics. We have

$$\rho(E^*,J) = \rho(E^*)\cdot\rho(J) = \rho_0\cdot\exp[2(a\cdot U)^{1/2}]\cdot\rho(J) \quad (2a)$$

where $\rho(E^*)$ and $\rho(J)$ separately describe the dependence of the level density on energy, E^*, and angular momentum, *J*.

In eq 2a, ρ_0 is a constant, the quantity *a* indicates the "level density parameter", and *J* is the angular momentum of the nucleus. For an explanation of the energy, *U*, in eq 2a, see below.

The angular momentum component $\rho(J)$ of eq 2a reads

$$\rho(J) = (2J + 1)\cdot\exp[-J\cdot(J + 1)/b] \quad (2b)$$

which means that the very large number $\rho(E^*)$ of levels per unit of excitation energy could be reduced with appropriate $J > 0$ by the factor $\rho(J)$. Roughly, the larger the value of *J*, the smaller the total $\rho(E,I)$, at least for light nuclei. If $A = 14$, $\rho(J) < 1$ for $J \geq 3$, whereas in heavy nuclei, a reduction of the angular momentum results for very large *J* only.

In eq 2b, the quantity *b* (roughly a constant, a "spin distribution parameter") contains the rotational moment of inertia of the nucleus. Prefactor $(2J + 1)$ in eq 2b and product $J\cdot(J + 1)$ in the exponent indicate that rotations of the nucleus are indeed concerned, the energies of which are calculated as "eigenvalues" (expectation values) of an angular momentum operator.

High-level density and large number of nucleons allow description of a nucleus as a gaslike system. The CN may be treated as a degenerate Fermi gas, that is, as a system of independent particles moving in a rather simple (square) potential, provided that $E^* \ll e_F\cdot A^{1/3}$, where e_F is the Fermi energy of a nucleus, $e_F \approx 33$ MeV (compare ref 6, p 224). Assuming that $A = 100$, we have $e_F\cdot A^{1/3} \approx 150$ MeV. We will consider in the following only excitation energies, E^*, of at most 15 MeV to meet the condition $E^* \ll e_F\cdot A^{1/3}$ safely.

To satisfy these conditions as far as possible with a conventional model, we will apply in Section 4 the thermal conductivity of a two-atomic gas but apply in the corresponding expressions (see later, eqs 5 and 6) properties of single nucleons (Fermions) for description of the conduction properties of nuclear matter in a rough approximation.

Accordingly, for the nucleons to be described as a Fermi gas, we have to subtract from E^* pairing energies, *P*, of neutrons and protons so that *U*, the energy available after splitting pairs of nucleons into independent particles, reads $U = E^* - [P(N) + P(Z)]$. Such an "independent particle" model (the Fermi gas) naturally is not valid at arbitrarily high excitation energies because it is the formation of the CN itself that shows that all nucleons of this system really become strongly coupled. Energy exchange between the

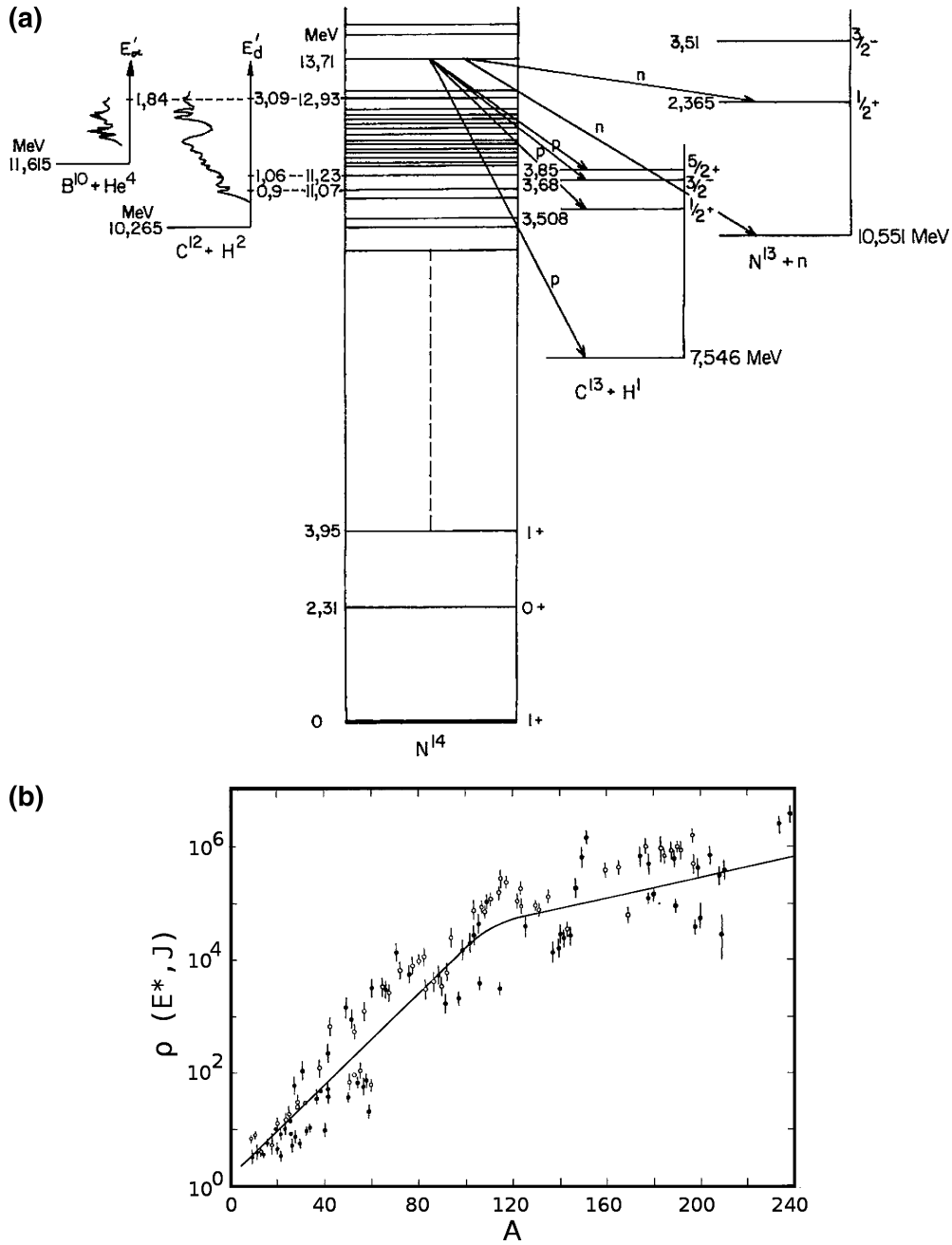

Figure 2. (a) Energy levels (schematic) of a compound nucleus. The nucleus, ^{14}N (central part of the Figure), excitation functions measured in the entrance channels, ^{10}B + ^{4}He and ^{12}C + d (left), and energy levels in two decay channels, ^{13}C + p and ^{13}N + n (right; n and p indicate neutrons and protons, respectively), are described. The Figure is taken from ref 5. Vertical directions in the diagrams indicate energy scale, E (excitation energy E^*) or $E_{\alpha'}$ or E_d' (kinetic, laboratory energy in the excitation functions measured with incident α particles or deuterons, d, and the corresponding target nuclei), both energies given in MeV. In the right-hand diagrams, "spin" (angular momentum, e.g., $^1/_2$, $^3/_2$) and parity (positive or negative signs) of the residual nuclei states are also indicated. Arrows are used to identify transitions from highly excited levels of ^{14}N to the excitation levels of the residual nuclei by emission of n or p. Coincidence of resonances measured in the excitation functions with levels of the compound nucleus, ^{14}N, is schematically indicated. (b) Experimental values of the level density in nuclei. Data[7] are given in dependence of total number, A, of nucleons. The full line refers to eqs 2a and 2b and is calculated in ref 7 for $U = 7$ MeV.

constituents of a CN is so intensive that kinetic energy states of single nucleons cannot be considered to be independent of each other. This also means that excited states of the CN do not have their origin in excitations, just of a single nucleon in the field of the remaining A-1 other nucleons. Pairing energies are an important component in the already mentioned liquid drop model; these (presently empirical) corrections apply if the number of neutrons or protons is either even or odd. (In even/odd nuclei, the pairing contribution to the binding energy is zero.) To make the application of the thermal conductivity of a two-atomic gas an acceptable approximation, we confine the discussion in the following to nuclei with only small contributions of pairing energy to the total binding energy.

The thermodynamic nuclear temperature, T_{th}, is calculated from $T = (U/a)^{1/2}$. (See standard textbooks on statistical mechanics.) If we use a level density parameter, $a = A/7.5$ per MeV (ref 9), $A = 100$, and $U = 10$ MeV, then the exponent $\rho(E)/\rho_0$ in eq 2a is on the order 10^{10} and T_{th} amounts to about 0.87 MeV or 10^{10} K. Low-level densities in the same nucleus are located at the beginning of the continuum (Figure 2a) at an

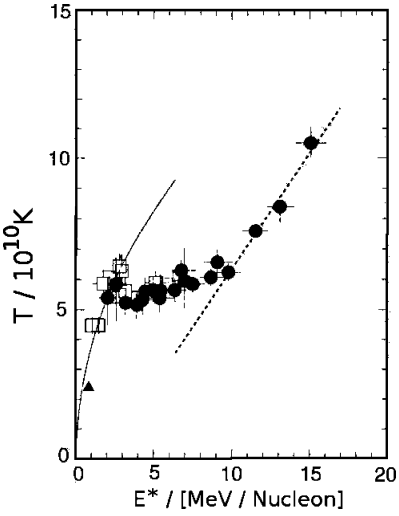

Figure 3. Nuclear temperature of heavy fragments produced in grazing collisions. Data[6] are obtained from measuring the collision between two ^{197}Au nuclei, which is dependent on the excitation energy per nucleon. Reprinted with kind permission of Springer Science + Business Media.

excitation energy of at least about 8 MeV, the binding energy of a single nucleon.

A very rough estimate is $\rho_0 \approx 10^{-2}$ per MeV for small J if $A = 100$. The level density $\rho(E)$ is then on the order of 10^8 per MeV, again using $U = 10$ MeV. Experimental values of $\rho(E,J)$ are illustrated in Figure 2b and are dependent on the number, A, of nucleons; the Figure is taken from ref 7, p 475. (Here the level density is reduced in comparison with the previous $\rho(E)$, which is, among other items, the consequence of a smaller energy, U). The $\rho(E,J)$ in Figure 2b increases to about $A = 100$. For heavier nuclei, the binding energy of a single neutron decreases from 8 MeV to about 5 MeV, which means that a heavy compound nucleus would be less excited than lighter nuclei, and its level density accordingly increases at a reduced rate.

Attempts to apply classical heat transfer processes, such as phase changes, to nuclear matter have become convincing because the temperature of nuclear fragments in high-energy collisions has recently been measured. (See Figure 3, taken from ref 6, p 327.) At low excitation energies, that is, at a temperature below $(5.5 \cdot 10^{10})$ K, there is a steep increase in nuclear temperature, as if the fragment had a classical specific heat. In an intermediate region, the temperature is almost constant (between $(5.5 \cdot 10^{10})$ K $\leq T \leq (6.5 \cdot 10^{10})$ K), which indicates that breakup of nucleon/nucleon binding and nuclear matter from a liquid droplet behavior transforms into a gaseous state. At high excitation energies, the temperature increases again. (At very high energies, a plasma of quarks and gluons can be investigated.)

Present interpretation by the same authors[6] is related to classical pool boiling: Above the liquid phase ($T > (5.5 \cdot 10^{10})$ K), a "gaseous" layer of loosely bound nucleons is formed around a condensed ("liquid") core of nucleons. The layer is not emitted but remains in equilibrium with the core and continuously exchanges nucleons until the whole core has reached the gaseous phase. Similarity to classical evaporation in pool boiling, perhaps with exception of the "layer", is obvious. Evaporation of nucleons will be more pronounced the higher the excitation energy of the nucleus.

In conclusion, there is apparently some similarity between nuclear and ordinary matter: We are thus allowed to speak of temperature and specific heat and entropy of a nucleus.

Returning to the α particle as a decay product, release of the binding energy defines two different energy states of the CN, the energies before and after formation of the α particle. Accordingly, there are also two nuclear temperatures, T_{th}, of the CN. With the same number of nucleons, level density parameter, and excitation energies as before, T_{th} amounts to about $T_i = (1.005 \cdot 10^{10})$ K and $T_f = (1.967 \cdot 10^{10})$ K, respectively, in the initial (i) and final (f) states, still before emission. The high temperature at the hot spot (the corresponding position where the binding energy is released) could lead to particle evaporation before the CN has come to thermal equilibrium, as was already pointed out by Bethe.[10] We will neglect this reaction channel like other pre-equilibrium processes.

2.4. Direction of the Thermalization Process. The following two items mainly concern the numerical simulations described in Section 5. First, kinetic energy, E_{kin}, in the center of mass system supplied in the collision between projectile, A, and target, B, plus binding energy of the entrance channel ($A + B$) is distributed to A nucleons of the CN. Except for the very instant of the collision in the entrance channel, the distribution mechanism of the kinetic energy, E_{kin}, is the same as that for the binding energy, E_B, released after formation of the CN from A and B. Just as the CN cannot remember from which constituents it was formed, the CN, after having obtained thermal equilibrium, can distinguish between neither kinetic and binding energy contributions that were distributed during thermalization nor positive or negative (see below) amounts of released energy.

A second item concerns the direction of the thermalization process. In a compound nucleus reaction $A + B \rightarrow CN^* \rightarrow C + D$, the excited compound nucleus, CN*, is formed before, for example, an α particle, C, is emitted. (We have excluded direct reaction channels.) However, if we use the release of binding energy of an α particle as a probe to determine diffusivity, then the direction of the corresponding thermal sequence would be opposite to the direction by which the CN reaction proceeds (from high to lower excitation energy). In other words, does the distribution of binding energy released during the formation of the α particle proceed not only by the same mechanism but also on the same time scale as the distribution of kinetic and binding energies in the entrance channel $A + B$?

As mentioned, entrance and decay channels can be interchanged to yield the same compound nucleus with the same excitation energy. This means, in the reverse order, that the α particle could also be interpreted as a "projectile", C, that hits a target nucleus, D, to form the excited compound nucleus, CN*. Because the α particle has to deliver its nucleons to the CN* (otherwise thermalization could not be completed), it has to be dissolved in the nucleus, D. Accordingly, its binding energy has to be supplied by the kinetic energy of the channel $C + D$ (now the entrance channel, which is the reverse in time to the (previous) entrance channel $A + B$). The α particle, in this picture, absorbs a positive energy needed for its decomposition, but we may also say that it releases a negative binding energy, respectively. In the language of standard laser flash methods, there would be a negative heat pulse impinging on the sample, such as a sudden, pointlike evaporation of a small liquid drop that consumes heat from the target. The distribution mechanism is, of course, the same for positive or negative binding energies, which means numerical simulations can be performed in the usual way. Some more specifications to this discussion can be found in Appendix A1.

In this article, in the first approximation, the diffusivity will be determined as a quantity independent of temperature. This

means that no nonlinear effects have to be considered, which in turn also means that the magnitude of the released energy (the "heat pulse", positive or negative) is of no importance for the numerical simulation. (A lower limit is set only by the resolution of the numerical tool.) Later, we will discuss a possible correlation of the extracted diffusivity with level density, and because level density depends on energy or on temperature, there must be a dependence of the diffusivity of nuclear matter on temperature, too. A quantitative discussion of this dependency is not possible in the present article. However, we will try in Section 5 to qualitatively correlate diffusivity with level density.

3. Lifetime of the Compound Nucleus

Following again the scheme a−c of Section 1, we next have to discuss the "detector". It is the lifetime of the compound nucleus energy states. The lifetime of the CN is not a universal constant; instead, each of its very large number of energy levels, E_{CN}*, can be assigned a lifetime before decay (provided that its decay is allowed from conservation of energy, angular momentum, and parity).

Consider again in Figure 2a the continuum energy states of the ^{14}N compound nucleus. In general, these energy states are excited in resonance-like processes that can be visualized when excitation functions with slowly increasing, low particle energies in the entrance channel are measured. If the excitation energy of the CN just equals one of its virtual levels, then the result is a resonance-like formation of the CN and a corresponding large reaction probability or reaction cross section. Two examples of excitation functions are shown on the left of Figure 2a, one for the entrance channel, ^{10}B + ^{4}He, the other for the alternative, ^{12}C + d. Note the correspondence of resonances in both excitation functions with energy levels of ^{14}N, as schematically indicated in this Figure. The resonance at $E_d' = 3.09$ MeV (E_d' indicates the kinetic laboratory energy of the deuteron) is correlated with a virtual level at an excitation energy, E_{CN}*, given by eq 1 to be $E_{CN}^* = E_{cm} + Q = (12/14)\cdot 3.09 + 10.27$ MeV $\approx$ 12.93 MeV of the ^{14}N compound nucleus. The width of this level is about 40 keV. It could be excited in ^{10}B + ^{4}H as well, with energy, E_α', of α particles of 1.84 MeV by $E_{CN}^* = (10/14)\cdot 1.84 + 11.62$ MeV $\approx$ 12.93 MeV.

The instability of the CN, that is, its tendency to statistically form and emit decay products, results in an energy uncertainty of these states. Energy uncertainties are generally represented by a "width", Γ, of resonances.

The width can be understood from (a) a quantum-mechanical concept, with wave functions, operators, and their eigenvalues, or (b) heuristically, by consideration of coupling of nucleon dynamics with the energy uncertainty of the whole system. (In a quantum mechanical view, resonances are observed when wave functions of incoming particle and internal wave function in the nuclear potential match each other at the nuclear radius, with a horizontal tangent.)

For the quantum mechanical aspect, assume that a particular level of a nucleus at an energy, E, is described by a wave function (compare, e.g., ref 8, p 399)

$$\psi = \psi_0 \cdot \exp\{-i \cdot E \cdot t/[h/(2\pi)]\} \quad (3a)$$

In this expression, $i = (-1)^{1/2}$ and $h/2\pi$ is the Planck constant. If the probability of de-excitation of this level is included, then its wave function reads

$$\Psi = \Psi_0 \cdot \exp\{-i \cdot (E - i \cdot \Gamma/2) \cdot t/[h/(2\pi)]\} \quad (3b)$$

where the energy, $E - i\cdot\Gamma/2$, is now a complex number. The probability, W, that the level is undisturbed after a time, t, is proportional to the product ($\Psi\cdot\Psi^*$); the second factor is the complex conjugate of the function Ψ. Because $W = (\Psi\cdot\Psi^*)$ yields $\exp\{-\Gamma\cdot t/[h/(2\pi)]\}$, the factor Γ in units of $h/(2\pi)$ is the probability of decay per unit time or the reciprocal of the mean lifetime, τ, of the level. This means that the product $\Gamma\cdot\tau$ is proportional to $h/2\pi$, the uncertainty principle that correlates uncertainty of energy with uncertainty of time (or with lifetimes). Because of the finite lifetime of any level of nuclear excitation energy, the level does not exhibit a sharply defined energy. A bound level with a mean lifetime against γ decay of, for example, 10^{-12} s has an energy uncertainty (a width) of about 10^{-3} eV. This principle applies not only to excited states but also to ground states: They have a nonvanishing width because of a finite (but very small) probability of being transformed by fission, β decay, or other nuclear reactions.

Width, Γ, and lifetime, τ, cannot be measured simultaneously for the same nuclear level because the product, $h/2\pi$, is very small. For example, width has been measured in excitation functions for a number of excited levels of ^{14}N, such as the levels with E* between (11 and 13) MeV; their width is between (200 and 20) keV, respectively. But the mean lifetime is on the order of only 10^{-20} s, which is far below resolution of any presently imaginable experimental equipment that has to rely on sharply defined beam energy and focus of magnetic lenses, small thickness of target, and high quality detectors.

The only method of determining lifetimes of excited CN states, therefore, is by measurement of Γ and application of the uncertainty principle. This becomes a problem at high level densities or with high beam energies in the entrance channel: Under this condition, only a continuum is observed because the spacing, D, between neighboring resonances becomes very small (on the order of electronvolts). Intuitively, one would also say that width should become narrow with increasing energy, but the system is furnished with more and more open decay channels so that the "transparency" to tunnel the nuclear potential wall by decay products increases. This overrides a decrease in Γ that would follow solely from a decrease in D. At high excitation energy, $\Gamma \gg D$, and resonances can no longer be experimentally resolved.

Widths of resonances obtained from measurement of excitation functions accordingly constitute the "experimental values", which are obtained at comparatively low incident beam energy in the excitation function, to which results of the numerical simulation reported in Section 5.3 will be fitted. In a numerical simulation of the thermal diffusion process, after release of a heat pulse (formation of the α particle or of any other particle composed of more than one nucleon), we look for the time interval, Δt, needed to obtain thermal equilibrium simply by calculation of the time interval that the sphere needs to arrive at vanishing energy or nuclear temperature differences, $\Delta E(\mathbf{e}) \rightarrow 0$ or $\Delta T(\mathbf{e}) \rightarrow 0$, respectively, for any location of the radius vector, $\mathbf{e}$, in its total volume.

A comparatively long lifetime for decay of the CN of approximately 10^{-16} s results from small widths of resolved CN resonances (Γ on the order of electronvolts) observed, for example, with slow neutrons. At increased beam energies, the lifetime is reduced to about 10^{-20} s, which corresponds to much larger Γ on the order of kiloelectronvolts to megaelectronvolts. This means that energy states excited from low beam energy decay more slowly than their counterparts located at increased excitation energy.

The question now is whether the result of the simulation, Δt, to obtain $\Delta T(\mathbf{r}) \rightarrow 0$, correlates with long ($\tau = 10^{-16}$ s) or short ($\tau = 10^{-20}$ s) lifetimes of excited nuclear states. If it

correlates, we can extract the diffusivity, κ, that is appropriate to fit the Δt to the τ. But does the Δt from the diffusion model have anything to do with the τ obtained from the width of resonances and application of the uncertainty principle?

To make this more transparent, we, in the following, address the heuristic point of view.

As a continuum model, diffusion cannot account for the generation or existence of discrete structures in any medium and under any gradient (temperature, concentration, or magnetic induction, to give some examples). This means that applicability of diffusion methods to a CN is not allowed if there are only bound states in a nucleus or the level density would be small. However, applicability improves and finally becomes justified if we focus the simulation on level densities that are large enough to consider the sequence (the spectrum) of excited states to be a continuum. In this case, necessarily, the dynamic energy states (velocities, v) of the nucleons also approach a continuum because it is the dynamic behavior of all nucleons that is responsible for the generation of a composite, the continuum of energy levels. At the beginning of thermalization, the velocity distribution of the nucleons is chaotic, but the dynamical behavior of the whole system becomes more Maxwellian the more we approach thermal equilibrium. The situation is like that in a classical gas: The higher its temperature, the better is the thermal conduction described by energy transfer in stepwise (short-range) interactions (collisions) between its components, that is, by a diffusion mechanism under a temperature gradient. Assume that the gas is enclosed between positions $x_1 \leq x \leq x_2$. Under stationary heat flow without internal heat sources, no maximum or minimum values of temperature (no quasi-discrete structure) can exist within $x_1 < x < x_2$, which means that the temperature gradient at any position, x, is not zero. Instead, as soon as the CN reaches thermal equilibrium, the dT/dx and, accordingly, the derivative dv/dx at fixed T' are zero at all positions $-R_{CN} < x < R_{CN}$.

Although the Maxwellian velocity distribution, $v(T')$, at a certain temperature, T', exhibits a maximum, v_{max}, exactly the same velocity distribution with the same v_{max} is observed everywhere in the CN where $T = T'$. This means that in a simple 1D picture, gradient dT/dx and, accordingly, derivative dv/dx at fixed T' are zero at all positions $-R_{CN} < x < R_{CN}$, under thermal equilibrium.

Starting with the initial event (projectile, A, hits target nucleus, B, in the entrance channel), we have extremely nonequilibrium conditions in the early stage of the system. In this situation, the CN is a continuum in neither velocity nor geometrical space; neither dT/dx nor dv/dx at fixed T' vanish anywhere in the CN. To arrive at thermal equilibrium, the CN needs a time interval, τ, which is necessary to achieve energetic (or temperature) homogeneity by ordering the initial chaotic velocity distribution to a Maxwellian distribution. Before ordering is completed, dynamics of the nucleons is reflected by an energy uncertainty, ΔE_{nucl}, given by their velocity distributions that are different at all $t < \tau$ and at all $-R_{CN} < x < R_{CN}$. The energy uncertainty of the nucleons is reflected by a corresponding energy uncertainty, ΔE_{part}, of emitted particles. It is this energy uncertainty that is seen as width, Γ, of the resonances simply because the resonances are measured by nothing other than the detection of the energy spectrum of particles emitted by the CN.

In summary of this subsection, there is a correlation between Γ, ΔE_{part}, ΔE_{nucl} and $dv(x)/dx$ of the Maxwellian distribution of nucleon velocities, and v correlates with temperature. Calculation of the time interval, Δt, needed to get $dv(x)/dx$ or $dT/dx = 0$ at all positions in the CN thus should allow extraction of the diffusivity necessary to fulfill this condition. There may be departures from a previously achieved equilibrium, such as emission of particles by which at least one nucleon is taken away from the CN or a group of nucleons "fuse" to a heavier decay product, at this instant. This means that the velocity distribution of the remaining nucleons has to be reordered to obtain a new equilibrium, Maxwellian velocity distribution, eventually before subsequent emissions or transitions take place in a cascade of events. In this picture, it is to be expected that the disturbance from equilibrium would be more serious and the t_E would consequently be extended the heavier the decay product or the higher the amount of energy and angular momentum carried away from the nucleus. The present analysis, accordingly, can also be understood as a departure from previously achieved equilibrium (compare Appendix A1).

Diffusivities, κ, extracted in Section 5.3, from the fit of numerical results to resonance widths or to the corresponding lifetimes accordingly must be classified with respect to level densities. At low level densities, the procedure cannot be reasonably applied. But lifetimes (via Γ and the uncertainty principle) and level densities are correlated at high level densities, and because lifetimes, when simulated by a numerical model, depend on diffusivity, κ, there must also be a correlation between κ and level density.

4. Thermal Diffusivity of Excited Nuclear Matter

4.1. Using Kinetic Gas Theory. For any spherical conductive system, Fourier's differential equation in spherical coordinates reads

$$\partial T/\partial t = k\cdot[(1/r^2)\cdot\partial/\partial r(r^2\cdot\partial T/\partial r) + (1/r^2\cdot\sin\theta)\cdot\partial/\partial\theta(\sin\theta\cdot\partial T/\partial\theta) + (1/r^2\cdot\sin^2\theta)\cdot\partial^2 T/\partial\varphi^2] \quad (4a)$$

where T is the temperature and r, θ, and φ are the radial, azimutal, and polar coordinates. If we allow a disturbance at arbitrary positions in the spherical volume, then it is not possible to reduce eq 4a to a simple radial dependence. (Only the polar component will vanish.) Thermalization of the CN shall be confined strictly to within its volume without interactions with neighboring nuclei.

Let a heat pulse, Q, of duration $\Delta t = 10^{-24}$ s be released within only a volume, V_α, the volume of an α particle. The duration of the pulse is, to some extent, arbitrary because in the present case, we do not start numerical simulation before the end of the pulse; it should be small just in comparison to the expected lifetimes. This defines the boundary condition

$$\begin{aligned} t = t_0: &\quad T(r \leq R_{CN}) = T_{CN}(t_0) = T_0 \\ t = t_1 = 10^{-24}\ \text{s}: &\quad T(V_{CN} - V_\alpha) = T_{CN}(t_1) = T_{CN}(t_0) \\ &\quad T(V_\alpha) = T_\alpha(t_1) = V_\alpha\cdot Q/(\rho\cdot c) \\ t \geq 0: &\quad \partial T/\partial r = 0 \quad \text{at} \quad r = R_{CN} \\ &\quad \text{(adiabatic conditions for all times, } t\text{)} \end{aligned} \quad (4b)$$

To solve eqs 4a and 4b, the diffusivity, κ, has to be known. We will first estimate κ from standard assumptions, but is the diffusion model applicable at all?

The thermal conductivity of a classical, two-atomic gas will tentatively be taken as a model for the conduction properties of nuclear matter. The assumption "two-atomic" shall account for pairing between protons and protons, or neutrons and neutrons, to zero angular momentum states of two nucleons in a nucleus. Pairing between nucleons is responsible for an

approximately constant ratio of binding energies per nucleon, at least if their number exceeds about $A = 30$; it also reflects a saturation property of nuclear force. Pairing of nucleons does not mean that this is a permanent coupling between two uniquely identified nucleons; instead, the partners may continuously change.

Further assume that the gas is infinitely extended and that it consists of symmetrical, small-field molecules. Small-field means that the molecules interact only when they come very close together (when surfaces touch each other), and the interaction then is repulsive, which is justified by the well-known short-range, repulsive component of the nuclear potential. Up to this point, one important aspect is missing in this model: the Pauli exclusion principle, but see below. Also, the assumption of an infinitely extended nucleus has to be justified later. Pairing does not mean that paired nucleons rotate like a gas molecule. There the two particles (atoms, ions) can be identified as long as the identity is not broken by scattering or absorption. Here the nucleons that form a pair cannot be identified and hence do not constitute a rotator with two centers of gravity.

Following Kennard, ref 11, equation 123, for a Maxwellian velocity distribution of the molecules that have just collided (i.e., under thermal equilibrium) and from eq 155c and chapter 104 in the same reference, the thermal conductivity, λ, for hard elastic spheres or classical point-mass (but two-atomic) molecules under any type of field is then given by

$$\lambda \approx (1 + \delta)\cdot(5/6)\rho\cdot c_v\cdot\langle l\rangle\cdot\langle v\rangle \qquad (5)$$

where δ is a small, positive constant ($\delta \leq 0.01$), ρ denotes the density of nuclear matter, c_v denotes the specific heat at constant volume, $\langle l\rangle$ is the mean free path between collisions, and $\langle v\rangle$ is the average molecule velocity. Comparison with low-temperature experimental data for the conductivity of two-atomic gases shows that the agreement is good (compare the table on p 180 in ref 11).

We will, in the following, take eq 5 of the conductivity of a classical gas for description also of the conduction properties of nuclear matter. The aim is to obtain at least an order of magnitude agreement with the few literature values available.

Strictly speaking (compare Tomonaga[3]), the nucleons should be interpreted as a gas mixed of quite different components, that is, protons and neutrons each with spin up or down that under pairing and coupling of spins form corresponding "two-atomic" nuclear molecules. The "spin", i, of a nucleon is the eigenvalue of its angular momentum, $i = {}^1/_2$, for neutrons or protons. Orientation of the spin vector is $+{}^1/_2$ or $-{}^1/_2$ with respect to a magnetic field (or up or down, in Tomonaga's model), but we simplify the model to an aggregate of only one sort of nucleons. All components of the model thus have the same definite density at all times. Note that this assumption (constant in time) may be too strong of a simplification: It is not clear that density is conserved in the early stages of thermalization. (There may be pre-equilibrium emissions that we have neglected.) Furthermore, contrary to Tomonaga's model,[3] it is rather questionable that we at all times have a Fermi distribution of energy states. Pairing of nucleons leads to the formation of states of even number of angular momentum to which a Fermi distribution no longer applies, except for high temperatures, and for which the mean free path might be increased, see below.

Medium density, ρ, of nuclear matter in its ground state amounts to about $(2.18\cdot10^{17})$ kg·m^{-3}. If we insert this value into eq 5, then the conductivity will be overestimated because the density in excited states of nuclei, such as in a compound nucleus, is certainly reduced, but the extent by which λ is overestimated in eq 5 when using ground-state density will be small because of the strong attractive component of the nuclear potential that prevents too strong of a blow up of the CN.

The specific heat, c_p, of excited nuclear matter is estimated from Figure 3 to about $(4.3\cdot10^3)$ J/(kg·K) using the nucleonic mass of $(1.675\cdot10^{-27})$ kg.

We provisionally could take the medium nucleon−nucleon distance as an estimate of the mean free path, $\langle l\rangle$, between particle/particle collisions in any stable nucleus; this amounts to $\langle l\rangle \approx (1.8\cdot10^{-15})$ m. An alternative and presumably better estimate is made from kinetic gas theory in that we take the radius of the specific property that is responsible for scattering of nucleons for energies below the Coulomb barrier: it is the charge distribution of the colliding particles. Accordingly, when taking the radius, r, of the charge distribution of the proton, $(0.862\cdot10^{-15})$ m (compare ref 6, p 81), the mean free path of a homogeneous Maxwellian gas of hard elastic spheres (ref 11, p 113, eq 106c,d)

$$\langle l\rangle = I/[\pi\cdot 2^{1/2}(2r)^2\cdot n] \qquad (6)$$

amounts to $(0.58\cdot10^{-15})$ m. In eq 6, n denotes the particle density, approximately $(1.3\cdot10^{44})$ nucleons·m^{-3}. As is to be expected, this estimate of $\langle l\rangle$ is significantly smaller than a medium nucleon−nucleon distance in a de-excited (stable) nucleus. There is a similar situation in scattering of light: The mean free path of photons in a dispersed medium is given by $1/E$ (with E the extinction coefficient); this can be significantly larger than the dimension of the scattering particles.

The radius, R_{CN}*, of a highly excited CN probably exceeds the radius, R, of the ground state of a stable nucleus with A nucleons

$$R_{CN}^* > R = r_0\cdot A^{1/3} \qquad (7)$$

In eq 7, $r_0 = (1.21\cdot10^{-15})$ m. For $A = 100$, we have $R_{CN}^* > (5.62\cdot10^{-15})$ m. The diameter of the CN (the clearance of the corresponding square potential walls) is thus about a factor of 20 larger than the mean free path, $\langle l\rangle$, which suggests that diffusion in a good approximation may be applied as model for the energy distribution mechanism in the CN; this also justifies the previously made assumption that the conductivity of an infinitely extended gas has been applied in eq 5. There will be no "gap" or temperature jump at the boundaries of the system. Another illustrative comparison with radiative transfer may be added. Although the CN is not infinitely extended, the ratio $\langle l\rangle/2R_{CN}$ of about 20 exceeds the limit for "optical thickness" $\tau_0 = 15$ in radiative transfer.[2] Neither radiation source nor boundaries can be identified if a layer of this thickness is between observer and source or boundary, respectively, because of the very small anisotropy of the scattered radiation. This means that radiative transfer, in this exceptional case, can be described as a diffusion process (and there is indeed a "radiative conductivity" that can be inserted into Fourier's conduction law).

Tomonaga[3] reports an increase in the mean free path of the nucleons caused by the Pauli exclusion principle. A single nucleon (with spin ${}^1/_2$) cannot assume a state (E,J) if this state is already occupied by another nucleon of the same energy and angular momentum. This also means that collision between both single nucleons is forbidden in this case. The number of possible collisions at low temperatures, accordingly, is reduced, which increases the mean free path, $\langle l\rangle$, of single nucleons, and the conductivity that results from eq 5 could be too small. However, as explained in ref 3, the increase in the mean free path scales with $1/T^2$ from the factor $[E/(k\cdot T)]^2$ where k is the Boltzmann

constant. At high temperature, the correction accordingly would be small. Furthermore, pairs of nucleons are not subject to the Pauli principle because their spin is an integral number.

Next, we need in eq 5 the average velocity, $\langle v \rangle$. A broad maximum observed in the scattering of high-energy electrons on H_2O targets (ref 6, p 83) confirms the fact that the nucleus is not a static ensemble of nucleons; instead, the nucleons move as quasi-free particles inside the potential of a nucleus. For an estimate of $\langle v \rangle$, we provisionally use the Fermi momentum, $p_F^2 = (5/3)\langle p^2 \rangle$, again a single particle quantity. For $A > 40$, it is almost constant, about 250 MeV/c (compare ref 6, p 224), where c is the velocity of light. We then have a mean velocity $\langle v \rangle$ of about $(6.2 \cdot 10^7)$ m·s^{-1} in the nucleus for single nucleons that we, as previously announced, as approximation insert into eq 5 for the two-atomic gas.

Then, as a first provisional result, we have $\lambda \approx (8.86 \cdot 10^{13})$ W·m^{-1}·K^{-1} from eq 5. This yields the thermal diffusivity

$$\kappa = \lambda/(\rho \cdot c_p) \approx (9.35 \cdot 10^{-8}) \text{ m}^2 \cdot \text{s}^{-1} \qquad (8)$$

of nuclear matter. This value of the diffusivity is approximately 30 % below the room temperature diffusivity of many classical nonconductors such as organic compounds. The small value of the diffusivity in relation to the enormous conductivity results from the very large density of nuclear matter.

4.2. Other Theoretical Models. The calculated value of κ can be compared with results reported by Weiner and Weström[12] when a link was established between pre-equilibrium and equilibrium phenomena and transport properties of nuclear matter. Assuming an initial excitation of a target localized within its finite volume, the authors consider a "hot spot" corresponding to momentum transfer in a collision, but they average over microscopic details of the nucleon scale by introducing local thermodynamics. The microscopic details, by analogy to the method applied in the present article, are contained solely in the diffusivity, κ, and the authors, too, apply eq 4a. Emission takes place from and normal to the surface of the excited nucleus: the higher the temperature, the more emissions will become possible.

Diffusion of heat then manifests itself not only in energy distribution but also in strongly anisotropic angular distribution of emitted nucleons. Therefore, if the nucleus exhibits an inhomogeneous temperature field, T (compare for illustration Figure 4a−c of the present article), then emitted nucleons carry with them some "local" information about that field (the larger T, the larger the relative probability to find evaporation products in a given range of scattering angles). Local temperature, accordingly, is determined[12] by observation of particle emission spectra, and the authors show that measurement of these distributions should provide direct information about heat conductivity of nuclear matter.

This theoretical method to determine the conductivity is rather different from that of the present article: We assume (to simplify the procedure) that the initial state (the hot spot) arises after overall equilibrium was obtained before the CN finally decays. Furthermore, the term "local" in ref 12 refers to a volume of which the radius is roughly given by the mean free path of the nucleons; the source thus approaches a pointlike geometry if compared with the size of the nucleus. In the present article, instead, the size of the α particle defines a small but finite volume of the energy source that is much larger than the mean free path, which seems to be more realistic.

The comparison of the results obtained from both methods for the diffusivity values will be made later (Table 1). A drawback of the method[12] is that it considers absolute values

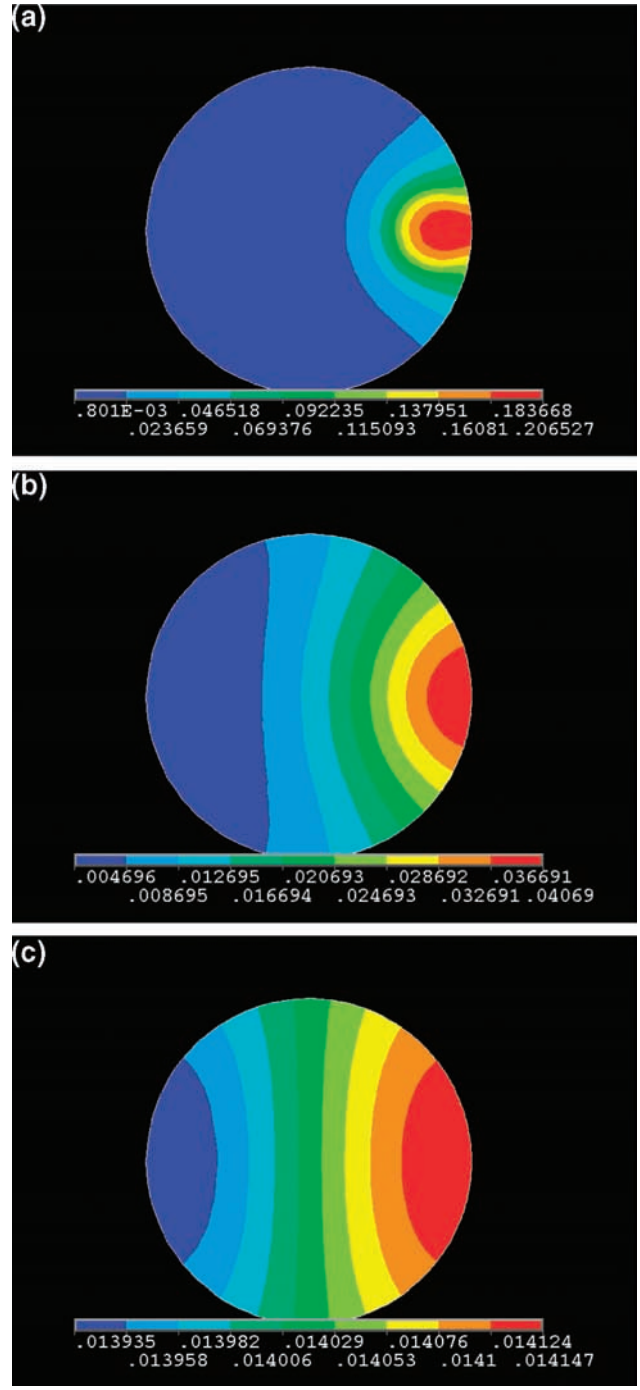

Figure 4. Contour diagrams of dimensionless temperatures, $\theta(\mathbf{e},t)$. Data are obtained in 3D finite element calculations showing the evolution with time, t, of temperature at positions inside the compound nucleus (CN) if formation of the α particle is near the periphery. The images result from a plane intersecting the centers of the α particle and the compound nucleus. Contours (from top to bottom) refer to $t = ((5 \cdot 10^{-23}), (1.5 \cdot 10^{-22}),$ and $10^{-21})$ s, respectively, for a nucleus with $A = 100$. The temperature interval is identified from the bar at the bottom of each image. At $t_1 = 10^{-24}$ s, the volume, V_α, of the α particle is uniformly at start temperature, $\theta(\mathbf{e},t_1) = 1$, whereas the volume, $V_{A\text{-}\alpha}$, is at zero relative temperature. At $t = 10^{-21}$ s (Figure 4c), variation of relative temperature in the whole CN volume is already between 0.01394 (outermost left) and 0.01415 (outermost right bar sections) and approaches zero, as displayed in Figure 6.

of temperature. Namely, the authors report that the temperature field decreases too fast with increasing time in regions where temperature, T, exceeds the equilibrium value, T_{eq} (and vice versa for regions where $T < T_{eq}$). Instead, from the numerical simulations of the present article, the diffusivity is extracted

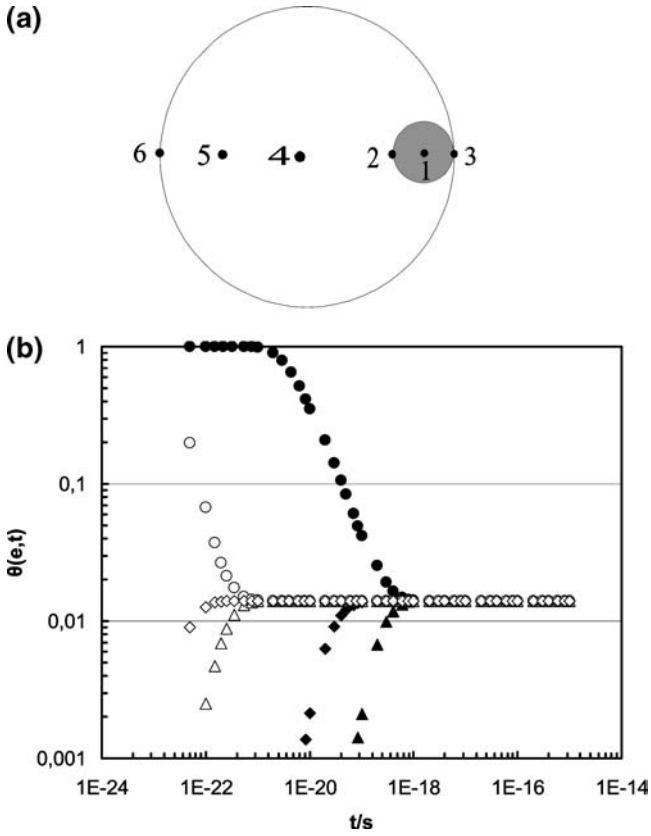

Figure 5. (a) Positons for calculation of evolution with time of dimensionless temperature, $\theta(\mathbf{e},t)$. Open and shaded spheres schematically represent the compound nucleus and the α particle, respectively. (b) Evolution with time of dimensionless temperature, $\theta(\mathbf{e},t)$. Results are plotted for the positions indicated in Figure 5a. At $t_1 = 10^{-24}$ s, temperature of the volume, V_α, of the α particle is uniformly set to $\theta(\mathbf{e},t_1) = 1$, whereas $\theta(\mathbf{e},t_1) = 0$ in the volume $V_{A\text{-}\alpha}$. The $\theta(\mathbf{e},t)$ values have been calculated using $A = 100$. Circles, tilted squares, and triangles denote positions 1, 4, and 6. Results obtained with for κ [10^{-8} m^2•s^{-1}] = 9.35 (open symbols) refer to high- (continuum) level densities, and results for κ [10^{-8} m^2•s^{-1}] = 9.35•10^{-3} (full symbols) can only provisionally, not quantitatively, be assigned to states of lower level densities. Time intervals, $t_{E,he}$ and $t_{E,le}$, needed to obtain thermal equilibrium are located approximately at $t = 8\cdot10^{-20}$ s and between (4•10^{-17}) s and (4•10^{-16}) s, for the high and low diffusivity values, respectively. (Compare the star and the two crosses on the abscissa in Figure 6.)

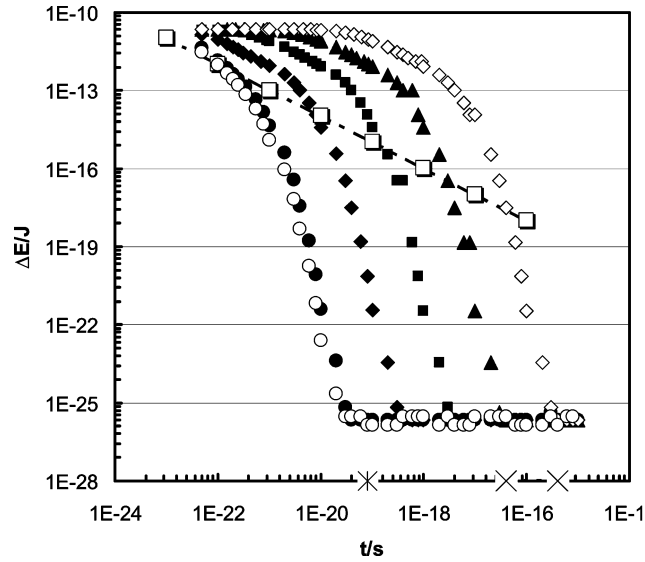

Figure 6. Evolution with time of maximum energy variation, ΔE_{max}, during thermalization. The Figure serves for extraction of the diffusivity, κ, by estimating the times, $t_{E,he}$ (*) or $t_{E,le}$ (×), for high- (continuum) and, only qualitatively, low-level densities until thermalization (saturation at $\Delta E \approx 10^{-26}$ J) is completed. The outermost left curves with ● and ○ refer to κ [10^{-8} m^2•s^{-1}] = 9.35 for $A = 100$ and 150, respectively. Identification of the other curves (all with $A = 100$) from left to right, is by κ [10^{-8} m^2•s^{-1}] = 0.935, 0.0935, 0.00935, and 0.000935, respectively. Shaded open squares denote the variation, ΔE, that results from the uncertainty principle, $\Delta E^*\Delta t \geq h/2\pi$, for given Δt.

from the maximum temperature difference and its convergence to a stationary value, but the idea of determining surface temperature by observation of particle emission spectra is fine.

Returning to the applicability of eq 5, the average velocity, $<v>$, of a pair of nucleons might be smaller than $<v>$ of single nucleons, the above estimate of λ and κ then provides upper limits for both quantities and, correspondingly, a lower limit for the time interval needed for thermalization, provided the mean free path $<l>$ is a constant. (We will come back to this point in Section 5.)

5. Time Needed for Thermalization by Diffusion

5.1. Results Obtained Using Diffusivity, κ, Obtained from the Gas Model. As before, we consider a CN consisting of $A = 100$ nucleons, and an α particle is condensed near the periphery of the CN. The radius of a free α particle (after release from the CN) is about (1.6•10^{-15}) m. This is still about one-third of the radius of the CN, which is not very suitable to treat the α particle as a point source located within the compound nucleus.

The formation of the α particle delivers 28.29 MeV as binding energy to the CN. Until a time t_1, this energy will be taken up by only these four nucleons. This means that we can assign the volume source, V_α, that the four nucleons occupy to a start temperature, $T_\alpha(t_1)$. The initial temperature of the remaining volume, $V_{CN\text{-}\alpha}$, of A-4 nucleons still is $T_{CN}(t_0) = T_0$. (Strictly speaking, the CN comprises not A-4 but A nucleons, but this has little impact on the final result if A is large.)

Dimensionless temperature, $\theta_{CN}(\mathbf{e},t)$, is defined by

$$\theta_{CN}(\mathbf{e},t) = T_{CN}(\mathbf{e},t)/T_{CN}(t_1) \qquad (9)$$

with the vector, **e**, previously defined.

Calculation of $\theta_{CN}(\mathbf{e},t)$ was performed by finite elements (FE). Free meshing was applied to the two spheres, V_α and $V_{A\text{-}\alpha}$. Because the FE program would interpret a sphere with a radius on the order of 10^{-15} m to be zero volume, appropriate scale transformations of length and time had to be applied. Fine meshing was made with 10-node, tetrahedral volume elements. The FE calculations cannot make reference to discrete structures such as individual energy levels or level densities and their properties, in particular, their angular momentum. This problem would require redesign of eq 4a in terms of transport properties of nuclear matter that specifically depend on angular momentum; this modification is presently not available, and it is even questionable whether it could be accomplished in a diffusion model. The difference between excitation energies of levels of same J will increase (simply, there are less states per mega-electronvolt if J becomes large, compare eqs 2a and 2b), contrary to the imagination of a continuum of energy states. Nonexistence of an energetic continuum also means that the imagination of a dynamical continuum in a nucleus fails, which means that the mean free path between nucleon/nucleon collisions in the CN would become too large for modeling the corresponding transport process as diffusion.

Table 1. Diffusivity, κ, of Nuclear Matter Obtained with Different Methods[a]

number A of nucleons	$\kappa/[10^{-8}\ m^2 \cdot s^{-1}]$ from $\chi(T_{eq}) \cdot \tau_0/R^2 = 0.118$		reference
100	13.24		12
	$\kappa/[10^{-8}\ m^2 \cdot s^{-1}]$ numerical, at high level density	$\kappa/[10^{-8}\ m^2 \cdot s^{-1}]$ standard, from two-atomic gas model	
100	$\approx 10 \pm 3$	9.35 ± 2.97	this work

[a] Dimensionless diffusivity, $\chi \cdot \tau_0/R^2$, from table 1 of ref 12 has been transformed into $\kappa/[m^2 \cdot s^{-1}]$ using $\tau_0 = (3 \cdot 10^{-23})$ s and $R = (5.802 \cdot 10^{-15})$ m for $A = 100$, as given in this reference. (There, original χ values were evaluated at equilibrium temperature, T_{eq}.) The κ obtained in the present work applies to the high density of nuclear levels, with $\rho(E)/\rho_0$ in eq 2a on the order of 10^{10}, assuming a nucleus with $A = 100$ and $U = 10$ MeV.

Results obtained from the numerical simulations of the dimensionless, transient temperature fields, $\theta_{CN}(\mathbf{e},t)$, are plotted as contour diagrams in Figure 4a−c. Temperature intervals are identified from the bar sections at the bottom of each Figure. Start temperatures at $t_1 = 10^{-24}$ s (Figure 4a) are $\theta(\mathbf{e},t_1) = 1$ (red bar section) in the volume V_α of the α particle and $\theta(\mathbf{e},t_1) = 0$ in the volume $V_{A\text{-}\alpha}$ (blue bar section). With increasing time, the temperature variation, $\Delta\theta(\mathbf{e},t_1)$, in the whole CN volume goes to zero and is below 1 % from the mean at $t \leq 10^{-21}$ s (Figure 4c).

Figure 5a,b shows temperature excursion with time, $\theta(\mathbf{e},t)$, of the CN during thermalization. The curves are obtained at the positions indicated in Figure 5a. Results shown in Figure 5b have been obtained with the value $\kappa = (9.35 \cdot 10^{-8})\ m^2 \cdot s^{-1}$ estimated in Section 4.1 with the two-atomic gas model (open symbols). This corresponds to high-level density ($\rho(E)/\rho_0$, on the order of 10^{10} and neglecting dependence on angular momentum) because only at high-level densities is diffusion meaningful, as previously explained. The corresponding continuum states necessarily are excited with high center of mass energy (he) in the entrance channel. At lower level densities, a tentatively used value, $\theta = (9.35 \cdot 10^{-11})\ m^2 \cdot s^{-1}$ (full symbols in Figure 5b), will be explained in the next subsection. (Presently, the indication "lower"-level density can only qualitatively be specified to "at least above beginning of the continuum".)

All curves in Figure 5b saturate at corresponding times, $t_{E,he}$ and $t_{E,le}$ (compare Figure 6), to the same value $\theta(\mathbf{e},t_E) \approx 0.014$, with very small temperature differences between any arbitrary positions, **e**.

5.2. Extraction of Diffusivity, κ, from Time, t_E, to Reach Equilibrium. A maximum temperature variation, $\Delta\theta_{max}(\mathbf{e},t)$, taken over the total spherical volume of the CN occurs at positions one and six, indicated in Figure 5a. From $\Delta\theta_{max}(\mathbf{e},t)$, the corresponding maximum energy variation, that is, the "uncertainty" $\Delta E_{max}(\mathbf{e},t)$, is obtained using

$$\Delta E_{max}(\mathbf{e},t) = \Delta\theta_{max}(\mathbf{e},t) \cdot T_{th}/k \qquad (10)$$

where T_{th} is the absolute thermodynamic temperature and k is the Boltzmann constant. Results are shown in Figure 6.

First, all curves in Figure 6 saturate at $\Delta E_{max}(\mathbf{e},t) \approx 10^{-26}$ J. Saturation at this level of energy uncertainty yields an estimate of the time, t_E, after which thermalization is completed. Using for the diffusivity, θ, the two-atomic gas value from Section 4.1, $\kappa = (9.35 \cdot 10^{-8})\ m^2 \cdot s^{-1}$ (the outermost left curves in Figure 6), we can extract $t_{E,he} \approx (8 \cdot 10^{-20})$ s (the star on the abscissa). For lower level densities, we have tried to extract $t_{E,le}$ from interpolation between two neighboring curves (▲ and ◇) that correspond to $\kappa = ((9.35 \cdot 10^{-11})$ and $(9.35 \cdot 10^{-12}))\ m^2 \cdot s^{-1}$, respectively. As a result, we obtain $(4 \cdot 10^{-17})$ s $\leq t_{E,le} \leq (6 \cdot 10^{-16})$ s.

5.3. Comparison of the Results with the Uncertainty Principle. We now compare the numerical solutions, $\Delta E_{max}(\mathbf{e},t)$, with the uncertainty, ΔE, that results from the uncertainty principle, $\Delta E \cdot \Delta t \geq h/(2\pi)$. (For a given lifetime, Δt, the ΔE resulting from this principle is illustrated by the shaded open squares in Figure 6.)

Rough agreement is seen over the whole interval of lifetimes. For a comparatively large width, $\Delta E = 10$ keV $= (1.602 \cdot 10^{-15})$ J, the uncertainty principle predicts a lifetime Δt of about $(6.6 \cdot 10^{-20})$ s, whereas extraction of the lifetime $t_{E,he}$ from the curve for $\kappa = (9.35 \cdot 10^{-8})\ m^2 \cdot s^{-1}$ (● or ○) yields $(8 \cdot 10^{-20})$ s, which is not a bad agreement. For a very small width $\Delta E = 1$ eV, we have a Δt of $(6.6 \cdot 10^{-16})$ s, whereas the curves for $\kappa = ((9.35 \cdot 10^{-11})$ and $(9.35 \cdot 10^{-12}))\ m^2 \cdot s^{-1}$ (▲ and ◇, respectively) yield $t_{E,le}$ between $((4 \cdot 10^{-17})$ and $(6 \cdot 10^{-16}))$ s.

Because the nuclear radius, R, in eq 7 depends only weakly on the number of nucleons, A, we expect little dependence of lifetime and extracted diffusivity on dimensions of energy source and spherical volume of the CN. For example, if we increase A from 100 to 150, then the nuclear radius increases by about 15 %. This means that thermalization would take longer and $\Delta\theta_{max}(\mathbf{e},t)$ would, accordingly, be increased at fixed time. However, the effect is small, as can be seen from the comparison of outermost left curves (● and ○ circles) in Figure 6.

From both comparisons, it appears that the diffusivity at highly excited states (large width, Γ, small lifetime) with correspondingly high-level density ($\rho(E)/\rho_0$ on the order of 10^{10}) to some extent could be larger than that expected from the classical model (the two-atomic gas, $\kappa = (9.35 \cdot 10^{-8})\ m^2 \cdot s^{-1}$). The diffusivity at lower level densities (corresponding to smaller widths, larger lifetimes) could still be smaller than the value $(9.35 \cdot 10^{-11})\ m^2 \cdot s^{-1}$ that was tentatively assumed in the previous subsection. An overall shift of the extracted diffusivities still results from interpretation of the Δt as maximum lifetimes; this generally would reduce the diffusivities below the extracted values. An additional, possibly existing effect caused by pairing will be discussed in the next section.

6. Discussion and Error Estimates

First, the agreement between the diffusivity obtained from either the numerical simulation or the classical gas model is within 10 %.

A comparison between the results obtained in the present article with the diffusivity reported in ref 12 is shown in Table 1. The dimensionless quantities $\chi \cdot \tau_0/R^2$ given in Table 1 of this reference have been converted to $\kappa/[m^2 \cdot s^{-1}]$ using $\tau_0 = (3 \cdot 10^{-23})$ s and $R = (5.802 \cdot 10^{-15})$ m for $A = 100$, as given by these authors. Deviation is, at the most, 35 % between the κ obtained from $\chi(T_{eq}) \cdot \tau_0/R^2$ and the κ of the present article when using the two-atomic gas model. (When considering the numerical result, the agreement is better.)

Furthermore, Pelc and Kozlowski[13] reported diffusivity obtained in a study of second sound propagation in nuclear matter. They define $\kappa = \tau \cdot v_s^2$, with $\tau = R/c$, the nuclear relaxation time, of about 10^{-23} s, where R is the nuclear radius, c is the velocity of light, and v_s is the velocity of sound in a

Fermi gas. With $v_s \approx v_F/3^{1/2}$, they find $\kappa = (2.6 \cdot 10^{-8})$ m$^2 \cdot$s^{-1}. This value seems to be confirmed when the authors compare the viscosity, η, of nuclear matter obtained from $\eta = \kappa \cdot \rho$ with theoretical literature values, but agreement with the present results is only within a factor of about three.

Although we have found some qualitative agreement between lifetimes obtained from numerical simulation and uncertainty relation and from comparison with literature values, undiscovered problems could be hidden in the numerically extracted diffusivity and the value estimated by using eq 8. The specific heat value, c, of nuclear matter was extracted as an experimental value from Figure 3. Differences between c_p, extracted from Figure 3, and c_v, to be used in eq 5, are negligible and cannot introduce large uncertainties. Density, ρ, at the highly excited states could only be smaller than the density of the ground state. Accordingly, from eq 8, one would expect an increase in the diffusivity with respect to possible uncertainties in c_v and ρ if conductivity, λ, is constant. It is therefore left to the conductivity to explain whether the observed agreement is by mere accident or has some physical background.

Diffusivity, $\kappa = \lambda/(\rho \cdot c_p)$ scales with the product $\langle l \rangle \cdot \langle v \rangle$ of mean free path, $\langle l \rangle$, and average velocity, $\langle v \rangle$, because in an infinitely extended gas, $\lambda \approx \rho \cdot c_p \cdot \langle l \rangle \cdot \langle v \rangle$. This means it is $\langle l \rangle$ or $\langle v \rangle$ (or both) that could introduce uncertainties in λ and κ.

A decrease in the mean free path, $\langle l \rangle$, means that the radius, r_{si}, of the "sphere of mutual influence"[10] would have to be increased. This can be due to attractive nuclear and repulsive Coulomb potential components. Charge independence of nuclear forces predicts that the nucleon−nucleon scattering cross sections (n,n or p,n or p,p) are equal. Accordingly, there is no definite need for variations of the radius, r_{si}, by assuming stronger nucleon−nucleon interactions between pairs in relation to the interactions between single nucleons. But the weakly interacting Coulomb potential becomes dominating when the distance between individual nuclei is larger than the range of the strong nucleon−nucleon force. Equation 6 then might not properly account for $\langle l \rangle$ because it simply assumes "hard" spheres, that is, particles that only in touch "feel" each other. However, although the Coulomb reaction parameter, for example, in $T(D,n)^4$He, is much larger than its fusion counterpart (compare standard textbooks on fusion technology), $\langle l \rangle$ of two-particle, ion/ion collisions in a plasma is on the order of several hundred meters, that is, large in comparison to plasma dimensions (which makes magnetic confinement necessary). By analogy, one would expect that the nuclear Coulomb potential cannot reduce $\langle l \rangle$ to values clearly below the CN radius.

However, if the average velocity, $\langle v \rangle$, of only part of single paired or unpaired nucleons would substantially be smaller, then the corresponding objects would more or less be at rest in relation to the fast movement of the others, which is contrary to experience. For example, quasi-elastic electron scattering, under the assumption of an impulse approximation (the electron in the scattering process interacts solely with a single nucleon), does not select fast nucleons and simply ignores the others (compare Figure 6.3 in ref 6, p 83). The nucleus is not a static entity with nucleons fixed to geometrical positions but is composed of quasi-free particles, none of which (regarding dynamic states) is preferred over the others. In other words, a strong reduction of neither $\langle l \rangle$ nor $\langle v \rangle$ seems to be meaningful.

When the uncertainty of the diffusivity as calculated using the gas model is estimated, the uncertainty in $\langle l \rangle$ without pairing corrections would be rather small, at the most by 10 %, because in eq 6, it relies on the radius of the charge distribution of the proton, which is known from experiments. However, the Pauli principle could increase this uncertainty to 30 % if a large percentage of nucleons were paired. Concerning $\langle v \rangle$, we have applied the Fermi velocity of single nucleons, which is safe within presumably 5 %, but a paring correction could double this uncertainty. With these very rough estimates, the total uncertainty in the diffusivity as obtained from the gas model is about $\pm (3 \cdot 10^{-8})$ m$^2 \cdot$s^{-1} if we assume that the different contributions enter the total uncertainty with equal weights.

The uncertainty in the diffusivity extracted from the numerical simulations stems from the uncertainty by which t_E is estimated in Figure 6 and from interpolation between neighboring curves. It is approximately the same amount as before, about 30 % of the extracted value. (As mentioned, the dependence of the temperature evolution on number of nucleons, A, is weak.)

But nuclear matter in some aspects also behaves like a liquid: The well-known liquid drop model allows predictions of binding energies, and the assumption of collective vibrations of protonic and neutronic liquids has successfully explained electric dipole giant resonances observed, for example, in photoinduced reactions. Nuclear matter could even behave like a quantum fluid, that is, have superfluidic properties like He(II), which, below the λ point, has a thermal conductivity that is about 10^8 times larger than that of the normal conducting LHe. Deviations from the rotation spectra of a deformed nucleus (considered to be a rigid rotator) or from the expected moments of inertia, too, indicate that nuclear matter exhibits some superfluidic properties. (The superfluid component of nuclear matter again correlates with pairing between nucleons.)

Accordingly, if the nucleus would not behave like classical condensed matter but some or even all nucleons would occupy superfluidic states, then one would expect higher λ and κ, in comparison with the values estimated in Section 4. Thermalization then would proceed on time scales substantially smaller than those obtained in the present simulations.

Yet one should not conclude that energy transfer in a CN cannot properly be modeled by diffusion. This would be contrary to the large value of $\langle l \rangle/2R_{CN}$, which is a strong indication of diffusion as a stepwise process. An integral, long-range energy exchange, such as the long-range, weak Coulomb potential or radiation, instead would slow down thermalization.

The existence of obstacles in the energy exchange processes would indicate increased viscosity of nuclear matter. Viscosity effects are well known in nuclei. Experimentally determined moments of inertia of a deformed nucleus are between values of the rigid rotator and a superfluidic liquid. Pairing, as the origin of a superfluidic component, would be responsible for zero internal friction and correspondingly reduce the moment of inertia, if a nucleus rotates. It is not clear that a superfluidic component normally responsible for vanishing viscosity of quantum liquids could now be the origin of unidentified obstacles in nuclear particle/particle collisions.

It is, of course, speculative to assume that it is not, or not only, the width of CN resonances that is an indicator for lifetime of the excited states. An answer, if needed at all, could be found only from theory and in future nuclear physics, not in heat transfer experiments. Presently, nothing speaks for a CN lifetime that significantly deviates from the traditional values.

In conclusion, the description of thermalization in nuclear matter by a diffusion process seems to be plausible. Calculated

and extracted diffusivity, apart from some unresolved uncertainties, is on the order of 10^{-7} $m^2 \cdot s^{-1}$ and certainly depends on level density. A quantitative specification of this dependence will be investigated in subsequent work.

7. Summary

Transient temperature excursion in a nucleus has been studied as an ideal case of a spherical, nontransparent heat-conducting volume and the time calculated after which the system reaches thermal equilibrium. From comparison with standard results for the lifetime of CN excited states and by application of the uncertainty principle, a tentative estimate of the diffusivity, κ, of nuclear matter can be reported. The diffusivity appears to depend significantly on nuclear level density (or excitation energy), a result that is not reported in previous literature. At high level density (i.e., $\rho(E)/\rho_0$ on the order of 10^{10}), it amounts to approximately 10 ± 3 in units of 10^{-8} $m^2 \cdot s^{-1}$ as a result of numerical simulations described in this article. This value of κ is confirmed by a classical, two-atomic gas model yielding $\kappa = 9.35 \pm 2.97$ in the same units if experimentally determined values are used for density and specific heat of nuclear matter and theoretical estimates for mean free path and average velocity of nucleons. These values are also roughly confirmed by theoretical models reported in the literature that applied completely different methods.

In conclusion, thermalization in nuclear matter again is confirmed to proceed by a diffusion mechanism, but the thermal transport properties of nuclear matter are profoundly different from conventional materials in that they also depend on excitation energy or energy level density. Instantaneous energy sources, instead of absorption of pulses from external sources, accordingly could be another candidate for determination of diffusivity of conventional materials on a laboratory scale.

Appendix A1

This additional information applies solely to the numerical method. Time reversal of the compound nucleus reaction can be exploited in the FE simulations on a more general interlevel (exchange of entrance and exit channels) and on an intralevel point of view. The first is concerned with overall specifications of the CN reaction, that is, with conservation of mass, energy, angular momentum, and parity, whereas the second is focused on only the direction of time within the exit channel, $C + D$.

The interlevel view simply helps to avoid the enormous problems involved if we had to analyze collision between incident beam and target particles in the entrance channel, $A + B$. Time reversal allows us to consider an exit channel, $C + D$, such as $^{13}C + p$ of the previous example (Figure 2a), as a hypothetic entrance channel, $A' + B'$, that reproduces ^{14}N (the same CN as before), which decays to a hypothetic exit channel $C' + D'$, such as $^{12}C + d$ (the reverse of the original entrance channel, $A + B$). This means that we can initiate and numerically analyze thermalization of the CN in entrance channels $A + B$ or $A' + B'$.

In the intralevel view, we, in principle, could analyze in positive ($A' + B' \rightarrow$ CN) or negative ($A' + B' \leftarrow$ CN) directions of the time arrow. (The latter simply coincides with $C + D$ of the interlevel scheme.) Whereas physics runs along with the second item (decay of a CN), the numerical simulation proceeds in the opposite direction (application of the FE program with negative time steps would cause useless problems), which means that we have to simulate ($A' + B' \rightarrow$ CN) to apply the FE tool. We start the analysis at a time t_1 and analyze the positive time interval, Δt, that is needed for thermalization to calculate the time $t_2 = t_1 + \Delta t$; this means that $t_2 > t_1$. In physical reality, however, $t_2 < t_1$ because the system, being excited in $A + B$, starts after having already obtained thermal equilibrium (t_2) for a decay to $C + D$. It is sufficient in the simulation to consider only the time interval Δt, whereas the absolute value of t_1 is arbitrary.

Symbols

Alphanumeric Symbols

A	number of nucleons in a nucleus
b	a constant in eq 2b that depends on the nuclear moment of inertia
c	velocity of light or specific heat
CN	compound nucleus
E	energy
h	Planck's constant
J	total angular momentum of the CN
k	Boltzmann constant
$<l>$	mean free path of a particle
LHe	liquid helium
p	momentum
S	entropy
t	time
T	thermodynamic temperature
$<\upsilon>$	average velocity of a molecule

Greek symbols

α	^4He
χ	dimensionless thermal diffusivity in ref 12
δ	a constant
κ	thermal diffusivity
λ	thermal conductivity
ρ	density
τ_0	optical thickness in ref 2 or nucleon mean free time in ref 12
Δ	difference

Superscripts

*	excited energy state of a nucleus or an excited energy level

Subscripts

B	binding
cm	center of mass property
eq	equilibrium
f	final
F	Fermi
he	high excitation energy (or high level density)
i	initial
J	total angular momentum
kin	kinetic
le	low excitation energy (or low level density)
p	pressure
si	indicates a sphere of "mutual influence", a term used in ref 11
υ	volume

Literature Cited

(1) Carslaw, H. S.; Jaeger, J. C. *Conduction of Heat in Solids*, 2nd ed.; Clarendon Press: Oxford, U.K., 1988.
(2) Reiss, H. Radiative Transfer in Nontransparent Dispersed Media. *High Temp.−High Pressures* **1990**, *22*, 481–522.

(3) Tomonaga, S. Innere Reibung und Wärmeleitfähigkeit der Kernmaterie. *Z. Phys.* **1938**, *110*, 573–604.
(4) Bethge, K.; Walter, G.; Wiedemann, B. *Kernphysik*, 2nd ed.; Springer Verlag: Berlin, 2001.
(5) Marmier, P. *Kernphysik II*, 5th ed.; Sheldon, E., Ed.; Verlag des Vereins der Mathematiker und Physiker an der ETH Zürich: Zürich, 1968.
(6) Povh, B.; Rith, K.; Scholz, Chr.; Zetsche, F. *Teilchen und Kerne*, 5th ed.; Springer-Verlag: Berlin, 1999, of which an English translation by M. Lavelle is available with the same authors: *Particles and Nuclei: An Introduction to the Physical Concepts*; Springer: Berlin, 1995, which, however, does not contain figure 19.6.
(7) Segrè, E. *Nuclei and Particles: An Introduction to Nuclear and Subnuclear Physics*; W. A. Benjamin: New York, 1965.
(8) Evans, R. D. *The Atomic Nucleus*; McGraw-Hill: Bombay, 1965.
(9) Facchini, U.; Saetta-Menichella, E. *Energ. Nucl.* **1968**, *15*, 54.
(10) Bethe, H. A. Possible Deviations from the Evaporation Model of Nuclear Reactions. In Proceedings of the American Physical Society, Minutes of the New York Meeting February 25−26, 1938. *Phys. Rev.* **1938**, *53*, 675 (only abstracts).
(11) Kennard, E. H. *Kinetic Theory of Gases*; McGraw-Hill Book Company: New York, 1938.
(12) Weiner, R.; Weström, M. Diffusion of Heat in Nuclear Matter and Pre-Equilibrium Phenomena. *Nucl. Phys.* **1977**, *286*, 282–296.
(13) Pelc, M.; Kozlowski, M. Second Sound in Nuclear Interaction. In *From Quarks to Bulk Matter*; Hadronic Press: Palm Harbor, FL, 2001, preprint available under miroslawkozlowski@aster.pl.

Received for review January 9, 2009. Accepted March 24, 2009.

JE9000334